Structural Basis of the Permeation Function of Plant Aquaporins

Sukanya Luang and Maria Hrmova

Abstract Aquaporins facilitate rapid and selective bidirectional water and uncharged low-molecular-mass solute or ion movements in response to osmotic gradients. The term 'aquaporin' was coined by Peter Agre and colleagues, who in 1993 suggested that major intrinsic proteins (MIPs) that facilitate rapid and selective movement of water in the direction of an osmotic gradient be named 'aquaporins (AQPs)' (Agre et al. 1993). Aquaporins are spread across all kingdoms of life including archaea, bacteria, protozoa, yeasts, plants and mammals. Plant aquaporins are classified within the ancient superfamily of MIPs, and based on sequence homology and subcellular localisation, they constitute several subfamilies. Genome-wide identifications of aquaporin genes are now available from around 15 plant species, and this information provides a rich source of sequence data for molecular studies through structural bioinformatics, three-dimensional (3D) modelling and molecular dynamics simulations. These studies have capacity to reveal new information, unavailable to X-ray diffraction studies of time- and space-averaged molecules confined in crystal lattices.

1 Summary

Aquaporins facilitate rapid and selective bidirectional water and uncharged low-molecular-mass solute or ion movements in response to osmotic gradients. The term 'aquaporin' was coined by Peter Agre and colleagues, who in 1993 suggested that major intrinsic proteins (MIPs) that facilitate rapid and selective movement of water in the direction of an osmotic gradient be named 'aquaporins (AQPs)' (Agre et al. 1993). Aquaporins are spread across all kingdoms of life including archaea, bacteria, protozoa, yeasts, plants and mammals. Plant aquaporins are classified within

S. Luang • M. Hrmova (✉)
School of Agriculture, Food and Wine, University of Adelaide, Glen Osmond, South Australia 5064, Australia
e-mail: maria.hrmova@adelaide.edu.au

F. Chaumont, S.D. Tyerman (eds.), *Plant Aquaporins*, Signaling and Communication in Plants, DOI 10.1007/978-3-319-49395-4_1

the ancient superfamily of MIPs, and based on sequence homology and subcellular localisation, they constitute several subfamilies. Genome-wide identifications of aquaporin genes are now available from around 15 plant species, and this information provides a rich source of sequence data for molecular studies through structural bioinformatics, three-dimensional (3D) modelling and molecular dynamics simulations. These studies have capacity to reveal new information, unavailable to X-ray diffraction studies of time- and space-averaged molecules confined in crystal lattices.

Aquaporins fold into a monomeric 'hourglass' or 'dumbbell-like' shaped structure that has been retained in all aquaporins. Individual monomers associate in vivo into functional tetramers, whereby this vertically symmetric structure provides foundation for residence within a lipid bilayer. Two plant aquaporin structures are available in structural databases (as of May 2016), which is that of (i) a predominantly water-permeable plasma membrane intrinsic protein (PIP) aquaporin in open and closed conformational states (PDB IDs: 1Z98, 2B5F and 4IA4) from *Spinacia oleracea* (Tornroth-Horsefield et al. 2006; Frick et al. 2013a, b) and (ii) an open state of a water- and ammonia-permeable tonoplast intrinsic protein (TIP) aquaammoniaporin from *Arabidopsis thaliana* (PDB ID: 5i32) (Kirscht et al. 2016). Detailed structural information on other plant subfamily members is now needed from economically important food plants such as wheat, barley, maize and rice, to provide strong foundations for future smart decisions directed to food production and sustainability.

Surprisingly, limited information is available on the solute permeation specificity determinants of plant aquaporins, although these data in conjunction with structural information are vital strategic tools for modifying their molecular function. Based on predominantly structural studies, it has been suggested that properties and steric occlusions of residues within the specific structural and functional elements are one of the most fundamental characteristics that underlie differences in transport selectivities of aquaporins. These main characteristics include (i) pore dimension parameters including their diameters and overall morphology; (ii) identities and flexibilities of residues lining solute-conducting pores; (iii) chemical configurations of pore constrictions in solute-conducting pores; (iv) properties of pore vestibules and a central pore, also dictated by the residues alongside the fourfold symmetry axis of tetramers; and (v) gating of aquaporins controlled by pH, cation binding, post-translational modifications such as phosphorylation and the dispositions of interacting loops.

We conclude that although structural aquaporin research has significantly progressed in recent years, many questions remain open. For example, are individual protomers within tetramers identical in function, what is the structural basis of permeation of non-electrolytes and ionic species, and the thermodynamic origin of transporting function of solutes, and how exactly have aquaporin proteins evolved during millions years of evolution into their current forms?

2 Aquaporins in Living Systems Including Plants

Plants acquire water from soil through aquaporins or use them as vehicles to dispose of excess of toxic substances (Schnurbusch et al. 2010; Hayes et al. 2013; Xu et al. 2015). Aquaporin molecules, amongst other pathways, are responsible for

hydraulic conductance of plants that underlies water uptake together with dissolved mineral nutrients (see also chapter "Plant Aquaporins and Metalloids"). Aquaporins facilitate rapid and selective bidirectional water and uncharged low-molecular-mass solute transport, in response to osmotic and concentration gradients, respectively. The latter does not necessarily rely on an osmotic gradient. This transport, occurring through polytopic aquaporins that span cell membranes, is independent of a supply of external energy (e.g. ATP). Thus, aquaporins are known to be passive transporters, although fundamental to their function are structural flexibility and gating, which may be dependent on the redox state of a cellular environment, on the activity of phosphorylation machinery (controlling the levels of, e.g. ATP) and on membrane and subcellular dynamics.

2.1 Aquaporins Occur in All Kingdoms of Life

Aquaporins are spread across all kingdoms of life including archaea, bacteria, protozoa, yeasts, plants and mammals. In archaea and bacteria, typically one aquaporin type is retained, while in eukaryotes gene duplications and horizontal gene transfer events have resulted in occurrence of subfamilies of aquaporins with diversified transport functions, although the canonical hourglass or dumbbell-like shaped architecture has been retained in all aquaporins. The typical examples of duplication and function diversification include aquaporins in fish, mammals and higher plants, in which neo-functionalisation has led to evolution of paralogous proteins with various solute selectivities, gating mechanisms or time and space differential expression (Fotiadis et al. 2001; Zardoya et al. 2002; Abascal et al. 2014). For example, 35, 35 and 39 aquaporins have been described in maize, *Arabidopsis* and rice, respectively (Chaumont et al. 2001; Johanson et al. 2001; Sakurai et al. 2005). These numbers are even higher in non-plant species such as in fish and some land vertebrates, due to several rounds of entire genome duplication during early stages of their evolution (Abascal et al. 2014), although most mammals only require the presence of limited numbers of aquaporins to properly function. Diverse aquaporin isoforms are directed to various subcellular locations and compartments and represent fundamental components for membrane evolution, diversity and differential gene expression. Through these specific membrane aquaporin-containing partitions, plants drive hydrostatic and osmotic forces that help them to maintain water homeostasis, together with hydraulic conductance in roots, stems and other organs (Fricke et al. 1997; Tyerman et al. 1999; Maurel et al. 2008; Chaumont and Tyerman 2014).

2.2 Plant Aquaporin Sequences and Their Genome-Wide Identification

Since the first member of the major intrinsic protein (MIP) family was described and its cDNA cloned (Gorin et al. 1984), the first plant MIP from soybean (nodulin 26) was identified (Sandal and Marcker 1988), along with the tonoplast intrinsic

protein (TIP) from bean seeds (Johnson et al. 1990), and α-TIP (Höfte et al. 1992) and γ-TIP (Maurel et al. 1993) from *Arabidopsis*, and other plants. Some of these proteins were described as water stress-induced proteins (Höfte et al. 1992) and only later functionally characterised as water channels. These discoveries were followed by a series of informative reviews on physiological function of aquaporins (e.g. Tyerman et al. 1999; Verkman and Mitra 2000; Gomes et al. 2009; Maurel et al. 2008; Chaumont and Tyerman 2014; Li et al. 2014; Mukhopadhyay et al. 2014). These physiological functions include photosynthesis, seed germination, cell elongation, stomata movement, reproduction (Reddy et al. 2015) and responses to a variety of abiotic stresses, such as anoxia (Choi and Roberts 2007), hydrogen peroxide toxicity (Dynowski et al. 2008; Wudick et al. 2015), mineral soil toxicity (boron and arsenic) (Isayenkov and Maathuis 2008; Ma et al. 2008; Kamiya et al. 2009; Schnurbusch et al. 2010; Li et al. 2011; Hayes et al. 2013; Xu et al. 2015), high salt (Zhang et al. 2008; Gao et al. 2010; Hu et al. 2012; Xu et al. 2013) and a low water potential drought (Xu et al. 2014; Li et al. 2015).

Genome-wide identification studies of aquaporin genes are now available from at least fourteen plant species, including *Arabidopsis* (Johanson et al. 2001), maize (Chaumont et al. 2001), rice (Sakurai et al. 2005), poplar (Gupta and Sankararamakrishnan 2009), grapevine (Shelden et al. 2009), cotton (Park et al. 2010), barley (Besse et al. 2011; Tombuloglu et al. 2015), soybean (Zhang et al. 2013), tomato (Reuscher et al. 2013) and bread wheat (Pandey et al. 2013). As a result of recent proliferations of genome sequencing initiatives, several new genome-wide identification studies were conducted in cabbage (Diehn et al. 2015), common bean (Ariani and Geps 2015), sorghum (Reddy et al. 2015) and wheat (Hove et al. 2015). These analyses have provided a rich source of sequence data information for molecular studies that have been conducted through structural bioinformatics (Wang et al. 2005; Deshmukh et al. 2015) and 3D structural (homology or comparative) modelling (Wallace and Roberts 2004; Schnurbusch et al. 2010; Gupta et al. 2012; Verma et al. 2015).

2.3 Classification of Aquaporins

Plant aquaporins are classified within the ancient superfamily of Major Intrinsic Proteins (MIPs) (Saier et al. 2016). Based on sequence homology and subcellular localisation, MIPs constitute five subfamilies, namely, plasma membrane intrinsic proteins (PIPs), tonoplast intrinsic proteins (TIPs), nodulin-26 intrinsic proteins (NIPs), small basic intrinsic proteins (SIPs) and X-intrinsic proteins (XIPs). In recent years, several studies have specifically focussed on molecular evolution and functional divergence of NIP (Liu et al. 2009) and XIP proteins (Bienert et al. 2011; Lopez et al. 2012; Venkatesh et al. 2015). These studies have pointed out that the functional divergence of various classes of aquaporins under selection pressures led to restrictions on the physicochemical properties of key functional amino acid residues, following gene duplication.

3 Three-Dimensional Structures of Aquaporins

3.1 Structural Information on Aquaporins Is Available from All Kingdoms of Life

3D atomic structures of aquaporins are accessible from archaea (Lee et al. 2005), bacteria (Fu et al. 2000; Savage et al. 2003; Savage et al. 2010), protozoa (Newby et al. 2008), yeasts (Fischer et al. 2009; Eriksson et al. 2013), plants (Fotiadis et al. 2000; Törnroth-Horsefield et al. 2006; Frick et al. 2013a, b; Kirscht et al. 2016) and mammals (Sui et al. 2001; Gonen et al. 2004; Harries et al. 2004), including humans (Murata et al. 2000; Viadiu et al. 2007; Horsefield et al. 2008; Ho et al. 2009; Agemark et al. 2012; Frick et al. 2014). For example, a sub-angstrom resolution structure of the *Pichia* water-conducting aquaporin (Eriksson et al. 2013) and a recent high-resolution structure of the *Arabidopsis* aquaammoniaporin (Kirscht et al. 2016) provided an unprecedented view into the landscape of positions of interacting residues and the mode of coordination of water molecules. The water positions that were defined with a high precision in a water-conducting pore (Eriksson et al. 2013), and definitions of tautomeric states of interacting Arg and His residues, provided an abundance of information on water molecule coordination at the entry of the channel. As a result of the availability of high-resolution aquaporin architectures of these structurally similar but functionally distinct MIP and TIP proteins, a plethora of theoretical in silico studies were initiated to investigate molecular dynamics of aquaporins and flow of solutes (Tajkhorshid et al. 2002; Wang et al. 2005; Cordeiro 2015; Han et al. 2015; Verma et al. 2015; Kitchen and Conner 2015). These studies revealed novel information, unavailable to studies of time- and space-averaged molecules confined in crystal lattices, and defined protein dynamics and energy barriers during permeation events of water, ammonia or other solute-conducting aquaporins (Wang et al. 2005; Han et al. 2015; Kirscht et al. 2016).

3.2 An Overall Architecture of Protomers

The 3D structures of aquaporins are highly conserved from archaea to humans. They consist of a circular α-helical bundle with a solute-conducting pore and cytoplasmic (intracellular) and periplasmic (extracellular) conical vestibules. Each monomer is formed by six tilted (crossing angles between 25 and 40°) membrane-spanning α-helices (H1-H3 and H4-H6) and two re-entrant short α-helices (HB and HE) running in two repeats, with five interconnecting loops (LA-LE) that collectively form a right-handed α-helical bundle (Fig. 1). The arrangements of first (H1-H3 and HB) and second (H4-H6 and HE) bipartite segments, α-helices of which are significantly tilted in a membrane, follow a pseudo-twofold axis that runs

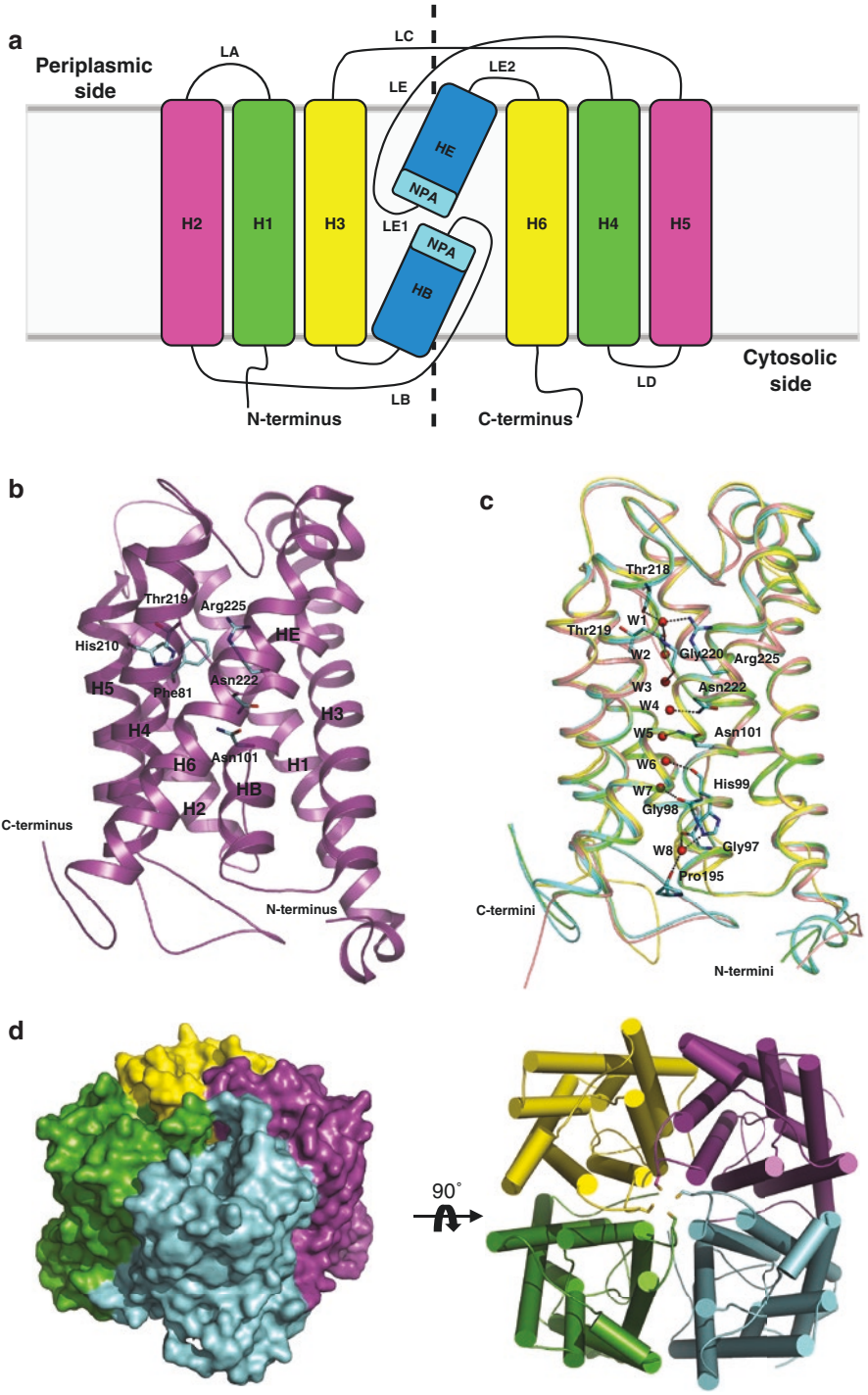
a
Periplasmic side
LA
LC
LE
LE2
HE
NPA
H2
H1
H3
LE1
NPA
HB
H6
H4
H5
Cytosolic side
LD
LB
N-terminus
C-terminus
b
Thr219
Arg225
His210
HE
H5
Phe81
Asn222
H3
H4
H6
Asn101
H1
HB
H2
C-terminus
N-terminus
c
Thr218
W1
Thr219
W2
Gly220
Arg225
W3
Asn222
W4
W5
Asn101
W6
W7
His99
Gly98
W8
Gly97
Pro195
C-termini
N-termini
d
90˚

perpendicularly to a membrane normal plane (Murata et al. 2000) (Fig. 1a; dashed line). In all aquaporins, N- and C-termini are cytoplasmically oriented (Fig. 1a). In some aquaporins, these termini are extended and carry sulfhydryl residues such as Cys (an inhibition site for mercury and other heavy metals) or N-glycosylation, phosphorylation and other post-translation modification sites.

3.3 A Circular Bundle and a Solute-Conducting Pore

The circular bundle of membrane-spanning α-helices encloses a solute-conducting pore (often referred to as a channel or a nanopore), which may be between 20 and 28 Å long and 4 and 6 Å in diameter. For example, in plant aquaporins, the pore narrows down around a selectivity filter region (defined below) (Törnroth-Horsefield et al. 2006; Frick et al. 2013a, b), or remains more uniform throughout the channel (Kirscht et al. 2016), but widens in all aquaporins to conical vestibules at both cytoplasmic and periplasmic sides (Fig. 1b).

A consensus, based on around 20 atomic structures of aquaporins, stipulates that the aromatic selectivity filter represents the narrowest constriction, at least in orthodox (predominantly water conducting) aquaporins (Fu et al. 2000; Sui et al. 2001). The selectivity filter is one of the most important regions underlying aquaporin specificity and represents as a package of four residues positioned near the periplasmic side of the pore. The selectivity filter is about 8–9 Å away from the first Asn-Pro-Ala (NPA) motif and was named the aromatic/Arg (ar/R)/LE1-LE2 constriction region (Fig. 1b). More precisely, this ar/R/LE1-LE2 region consists of one residue each from H2 and H5 α-helices, and two residues positioned on loop LE, located at partitions LE1 and LE2 that flank the NPA motif (Figs. 1a and 2b) (Fu et al. 2000; Sui et al. 2001; Savage et al. 2003). In all solved spinach aquaporins in closed or

Fig. 1 (**a**) A membrane topology diagram of aquaporins. Each protein molecule consists of six transmembrane α-helices (H1-H6) and two re-entrant α-helices (HB and HE), with NPA motifs, shown as cyan boxes. Transmembrane α-helices are connected via five interconnecting loops (LA-LE), whereby partitions LE1 and LE2 flank the second NPA motif, separated by approximately 4–5 Å from the first NPA motif. A *dashed line* indicates bipartite structural repeats of an hourglass aquaporin fold. (**b**) A cartoon representation of the spinach aquaporin SoPIP2;1 in the closed conformation (PDB ID: 1Z98). The selectivity filter residues (Phe81, His210, Thr219 and Arg225) and the two conserved asparagine residues (Asn101 and Asn222) of the NPA motifs are shown as cyan sticks. N- and C-termini are indicated. (**c**) The superposition of SoPIP2;1 structures including closed states at pH 8.0 (PDB ID: 1Z98) and at pH 6.0 (PDB ID: 4IA4), an open state (PDB ID: 2B5F), and the structure with a mercury activation site (PDB ID: 4JC6), shown in *cyan*, *pink*, *yellow* and *green*, respectively. Residues that interact with a single file of water molecules W1-W8, shown as red spheres, are indicated in cyan sticks. Hydrogen bonds between residues and water molecules are shown in *dashed lines*. (**d**) Prediction of a tetrameric assembly of the spinach aquaporin SoPIP2;1 in two orthogonal orientations (*left and right* images are related by 90° rotation to the viewer), whereby cysteine residues (shown in sticks) from each monomer participate in a quaternary assembly

open conformations, protein folds and more specifically pores enclose a single-file chain of water molecules coordinated by surrounding hydrophilic amino acid residues (Fig. 1c, cyan sticks). Recently, the presence of a novel water-filled side pore was defined in the AtTIP2;1 aquaammoniaporin, which is assumed to play a role in

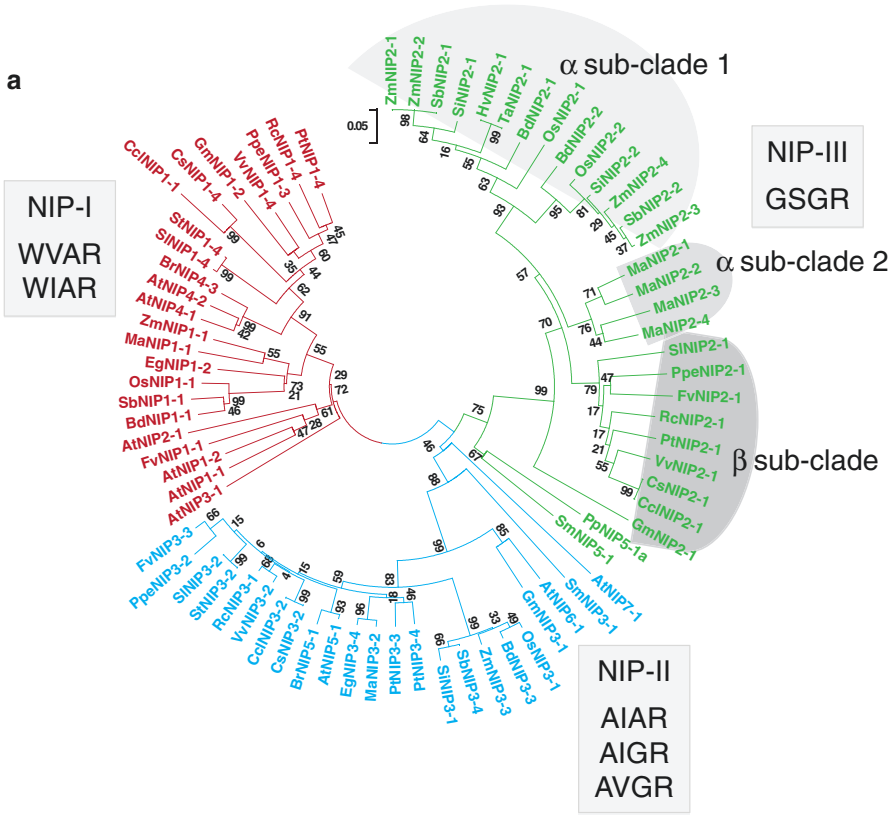

b

```
                          H2                          H5                    LE1   LE2
Conservation     5   7 5   97 7 5 675 55    7 657  69  6       57      67577995965979
SoPIP2-1         GSVGLLGIAWAFGGMIFVLVYCTAG    VPILAPLPIGFAVFMVHLATIP    ITGTGINPARSFGAAVIF
NIP-I
OsNIP1-1         GQITFPGVAIVWGLAVMVMVYAVGH    IGELAGLAVGATILLNVLIAGP    ISGASMNPARSLGPAMIG
GmNIP1-2         -SVTFPGVCVTWGLIVMVMIYSLRR    VGDFAGVAVGMTIMLNVFIAGP    VSGASMNPARSIGPALIK
AtNIP1-1         NVVTLPGIAIVWGLTIMVLIYSLGH    IGELAGLAIGSTVLLNVLIAAP    VSSASMNPGRSLGPALVY
ZmNIP1-1         GTVTFPGICAVWGLAVMVMVYSVGH    IGELAGLAVGATVLLNVLFAGP    ISGASMNPARTLGPALVV
AtNIP3-1         KPVTLPGIALVWGLVVTVMIYSIGH    TGSFAGIAIGATIVLDILFSGP    ISGASMNPARSLGPALIW
NIP-II
GmNIP3-1         GSETLIGCAATWGLAVMIVILATGH    VGELAGIAVGATVMLNILIAGP    VSGGSMNPVRTLGPAVAA
ZmNIP3-3         GAISPFGNAACAGLAVATVILSTGH    VGELAGIAVGAAVTLNILVAGP    TTGGSMNPVRTLGPAVAA
AtNIP5-1         GAETLIGNAACAGLAVMIIILSTGH    VGELAGIAVGATVMLNILVAGP    STGGSMNPVRTLGPAVAS
OsNIP3-1         GAISPFGNAACAGLAVTTIILSTGH    VGELAGIAVGAAVTLNILIAGP    TTGGSMNPVRTLGPAVAA
AtNIP7-1         GHVGLLEYAVTAGLSVVVVVYSIGH    LGNLTGFVIGTVISLGVLITGP    ISGGSMNPARSLGPAVVA
NIP-III
HvNIP2-1         TRISQLGQSVAGGLIVVVMIYAVGH    VGELAGLAVGSSVCITSIFAGA    VSGGSMNPARTLGPALAS
TaNIP2-1         TRISQLGQSVAGGLIVVVMIYAVGH    VGELAGLAVGSSVCITSIFAGA    VSGGSMNPARTLGPALAS
GmNIP2-1         RMVSKLGASLAGGLIVTVMIYSIGH    TGQLSGVAVGSSVCIASIVAGP    ISGGSMNPARTLGPAIAT
ZmNIP2-1         DRISQLGQSVAGGLIVTVMIYAVGH    VGELAGLAVGSAVCITSIFAGA    VSGGSMNPARTLGPALAS
OsNIP2-1         SRISQLGQSIAGGLIVTVMIYAVGH    VGELAGLAVGSAVCITSIFAGA    ISGGSMNPARTLGPALAS
```

ammonia deprotonation during permeation, as revealed by molecular dynamics simulations (Kirscht et al. 2016). In some aquaporins, a second well-formed constriction is located near to the cytoplasmic vestibule.

3.4 Cytoplasmic and Periplasmic Conical Vestibules

The cylindrical solute-conducting pore is flanked by two shallow, asymmetric vestibules. These are present on each side of the pore that flare into both cytoplasmic and periplasmic spaces and are formed by loop regions at each monomer face and by the N- and C-termini at the cytoplasmic face. The vestibules give a characteristic hourglass shape of aquaporin proteins (Fig. 1b). It was revealed that in nearly every atomic structure, these vestibules contain a contiguous chain of hydrogen-bonded molecules that extend from the surface of vestibules to either an ar/R/LE1-LE2 selectivity filter region of the periplasmic vestibule or to a second constriction near to the cytoplasmic vestibule (Fig. 1b).

3.5 Aquaporins Exist as Functional Tetramers

In native environments, individual monomers form a quaternary tetrameric assembly, in which homo- or hetero-oligomers that act as independent solute-conducting units associate with each other into a tightly fitting extended trapezoid or a

Fig. 2 (**a**) A phylogenetic tree of 75 NIP proteins from *Arabidopsis thaliana* (At), *Brachypodium distachyon* (Bd), *Brassica rapa* (Br), *Cajanus cajan* (Cc), Citrus clementine (Ccl), *Carica papaya* (Cp), *Citrus sinensis* (Cs), *Elaeis guineensis* (Eg), *Fragaria vesca* (Fv), *Glycine max* (Gm), *Hordeum vulgare* (Hv), *Musa acuminate* (Ma), *Oryza sativa* (Os), *Picea abies* (Pa), *Physcomitrella patens* (Pp), *Prunus persica* (Ppe), *Populus trichocarpa* (Pt), *Ricinus communis* (Rc), *Sorghum bicolor* (Sb), *Setaria italica* (Si), *Solanum lycopersicum* (Sl), *Selaginella moellendorffii* (Sm), *Solanum tuberosum* (St), *Triticum aestivum* (Ta), *Vitis vinifera* (Vv) and *Zea mays* (Zm). The tree was constructed by MEGA 6 (Tamura et al. 2013). A bootstrap analysis was performed with 1,000 replicates. Entries (Table 1) are clustered in the three independent clades NIP-I, NIP-II and NIP-III, each with specific selectivity filter signatures. NIP-I clade (in *red*): Trp-Val-Ala-Arg (WVAR) and Trp-Ile-Ala-Arg (WIAR). NIP-II (in *blue*): Ala-Ile-Ala-Arg (AIAR), Ala-Ile-Gly-Arg (AIGR) and Ala-Val-Gly-Arg (AVGR). NIP-III (in *green*): Gly-Ser-Gly-Arg (GSGR). Segregation of α (*lighter grey shades*)- and β (*darkest grey*)-sub-clades consisting of clearly distributed mono- and dicotyledonous sequences, respectively, is indicated. (**b**) A sequence alignment of α-helices H2 and H5 and loop LE of spinach aquaporins (SoPIP2-1) with NIPs from *A. thaliana* (AtNIP), *G. max* (GmNIP), *H. vulgare* (HvNIP2-1), *O. sativa* (OsNIP), *T. aestivum* (TaNIP2-1) and *Z. mays* (ZmNIP). The alignment was performed by ProMals3D (Pei and Grishin 2014). Selectivity filter residues and NPA motifs are shown in *blue* and *yellow*, respectively. Conservation of residues on a scale 5–9 from lower to higher conserved residues is displayed above sequences; 9 in *brown* indicates an absolute conservation

cylindrical wedge (Fig. 1d, tetrameric structures are shown in two orthogonal orientations). Monomers operate in their own right, as demonstrated by studies with mixed active or inactive monomers in *Xenopus laevis* oocytes (Jung et al. 1994). However, by close association, the four monomers form an additional central pore that has been suggested to serve as another route for permeation (Yool et al. 1996; Fu et al. 2000). Individual monomers are related by a fourfold crystallographic axis and interact with each other through neighbouring membrane-spanning α-helices via hydrophobic interactions and hydrogen bonds, such as those of 'hole-to-knob' configurations (Murata et al. 2000; Fu et al. 2000; Sui et al. 2001). Further, interconnecting loops between individual α-helices contribute to mutual inter-monomeric interactions (Fig. 1d, right panel). The tetramers associate with annular or exogenously added lipids, for example, with 1,2-dimyristoyl-sn-glycero-3-phosphocholine (Gonen et al. 2005) or surfactants such as octyl (Fu et al. 2000) and nonyl (Sui et al. 2001) β-D-glucosides, where both lipids and surfactants stabilise supramolecular tetrameric assemblies. These lipid or surfactant interactions have been defined in structures based on 3D (Fu et al. 2000) and two-dimensional (Gonen et al. 2005) crystals and are formed between hydrophobic residues and acyl chains of lipids or between glycosyl moieties of alkyl β-D-glucosides surrounding polar groups and water coordinated molecules. Occasionally, lipid molecules have been found in a central tetrameric pore, formed alongside the fourfold symmetry axis that can be up to 8–10 Å in diameter (Horsefield et al. 2008; Newby et al. 2008).

4 A Structural Basis of Transport by Aquaporins

4.1 Approaches to Measure Solute Transport Selectivity and Kinetic Parameters

Four mainstream approaches have been used to measure selectivity and kinetic parameters of solute permeation of aquaporins: (i) In isolated tissues (e.g. tobacco leaf discs; Uehlein et al. 2003), organelles of living organisms (e.g. endoplasmic reticulum, Noronha et al. 2014) or protoplasts (Ramahaleo et al. 1996; Moshelion et al. 2004; Besserer et al. 2012). (ii) In native vesicles isolated and purified from cells or their membranes (Niemietz and Tyerman 1997; Fang et al. 2002) or in vesicles isolated from membranes of cells with recombinantly expressed aquaporins (Jung et al. 1994; Schnurbusch et al. 2010). (iii) In *X. laevis* oocytes, used for the first time by Preston and co-workers (1992) and subsequently adopted by many researchers (e.g. Dordas et al. 2000). (iv) In liposomes with purified and reconstituted aquaporin proteins (proteo-liposomes) or planar lipid bilayers (Ye and Verkman 1989; Zeidel et al. 1992; Weaver et al. 1994; Verdoucq et al. 2008). Some authors argue that solute permeation measurements using proteo-liposomes are more reliable than those with oocytes (Ho et al. 2009), whereby in the absence of other proteins in a bilayer in the proteo-liposomes, precise kinetic permeation parameters can be derived for wild-type or variant aquaporins and compared. On the

other hand, proteins may not be accommodated in the membranes of proteo-liposomes in optimal configurations as these environments are artificial and minimalist in composition. Under ideal circumstances, both non-defined native and fully defined artificial systems should be used when available, for derivation of transport characteristics.

4.2 Solute Selectivity of Aquaporins

Based on permeation function, three major groups of plant aquaporins are recognised: (i) aquaporins that transport water, (ii) aquaglyceroporins that permeate other neutral solutes in addition to water (Borgnia et al. 1999) and (iii) aquaporins that conduct ionic species, based on the evidence of human aquaporins (Yool et al. 1996; Fu et al. 2000; Yu et al. 2006), as discussed below. The group of aquaglyceroporins has been reported to transport a broad range of neutral molecules such as non-electrolyte acetamide (Rivers et al. 1997); long polyols (Tsukaguchi et al. 1999); short polyols including glycerol (1,2,3-propane-triol) (Fu et al. 2000); CO_2 (Uehlein et al. 2003, 2008; Otto et al. 2010; Mori et al. 2014); purines and pyrimidines (Tsukaguchi et al. 1999); non-electrolyte urea (Liu et al. 2003); ammonia and glycerol nitrate (Loqué et al. 2005); silicic acid (Ma et al. 2006; Schnurbush et al. 2010); boric, arsenic and germanic acids (Takano et al. 2006; Kamiya et al. 2009; Schnurbush et al. 2010; Hayes et al. 2013); lactic acid (Choi and Roberts 2007; Bienert et al. 2013); hydrogen peroxide and related oxy-radicals (Dynowski et al. 2008); and selenious acid (Zhao et al. 2010). Although permeation of short and certain long (ribitol, xylitol, D-arabitol and D-sorbitol but not D-mannitol) polyols (Fu et al. 2000) has been detected in numerous studies, permeation of cyclic monosaccharides such as glucose and fructose, or of disaccharides such as sucrose, has never been demonstrated (Tsukaguchi et al. 1998; Fu et al. 2000).

4.3 Rates of Solute Transport and Mechanisms

Aquaporins as water transport facilitators mediate the water flux at rates of approximately $3{\cdot}10^9$ water molecules per second per monomeric unit (Agre and Kozono 2003); these rates are significantly higher than diffusion rates of water molecules through lipid membranes. In nonorthodox aquaporins that permeate other solutes, water transport rates are significantly lower. It has been suggested that steric occlusions of amino acid residues within specific structural and functional elements of aquaporins are one of the most fundamental factors that underlie differences in solute permeation selectivity (Fu et al. 2000; Lee et al. 2005; Kirscht et al. 2016). To this end, in the text below, we will separately discuss three features that collectively contribute to solute transport selectivity: (i) dimensional filtering and roles of periplasmic or cytoplasmic constrictions in permeation of solutes of various volumes;

(ii) chemical filtering of solutes, barriers for ion or proton conductance through pores of monomers and significance of NPA signatures, including roles of dipole moments and electrostatic potentials; and (iii) ion conductance through a central pore of tetramers.

4.4 Dimensional Filtering and the Roles of Constrictions in Permeation of Solutes of Various Volumes

A pathway for solute permeation is shaped by re-entrant α-helices HB and HE that connect to cytoplasmic and periplasmic vestibules, thus generating an hourglass or dumbbell-like shape (Fig. 1c). The solute-conducting channel, which in canonical aquaporins carries a single-file chain of water molecules, is formed by symmetry-related sets of carbonyl groups and hydrophilic side chain residues, both operating as hydrogen bond acceptors, often punctuated by hydrophobic residues alongside the pore. At the pore centre in most aquaporins, the two re-entrant α-helices HB and HE carry NPA motifs, where highly conserved Asn residues, rarely replaced by other residues (Zeuthen et al. 2013; Kirscht et al. 2016), and located at the tip of each re-entrant α-helix, form a part of the surface of the solute-conducting pore (Fig. 1c).

The sequence signatures of aquaporin monomers translated into the structural context underlie the functional properties of aquaporins. Verma et al. (2015) calculated a specific cumulative van der Waals volume (CvV, expressed in $Å^3$), by adding individual van der Waals volumes of each of the four residues of the ar/R/LE1-LE2 constriction, located close to the periplasmic vestibule. These authors noted large differences in CvV values in several subfamilies of aquaporins. For example, the largest CvV value was calculated for a mammalian aquaporin (ar/R/LE1-LE2 constriction region: Phe-Arg-Tyr-Arg) (572 $Å^3$), while the lowest CvV values were found for plant SIP (Ser-His-Gly-Ala) (306 $Å^3$) or protozoan (Ile-Ser-Gly-Ala) (312 $Å^3$) aquaporins (Verma et al. 2015). However, the ar/R/LE1-LE2 constriction regions Phe-His-Thr-Arg and Trp-Gly-Phe-Arg of the *E. coli* water-selective (AqpZ) and glycerol-selective (AqpF) aquaporins, respectively, exhibit identical CvV values (413 $Å^3$), so logically it is reasonable to conclude that besides chemical signatures and consequent structural importance of ar/R/LE1-LE2 constriction regions, other structural determinants that are not directly interact with solutes may play essential roles in solute permeation selectivity (Savage et al. 2010). Nevertheless, it might prove advantageous to investigate if additional quantitative parameters correlate with the solute permeation selectivity of aquaporins. The role of a cytoplasmic constriction, located in the proximity of the cytoplasmic vestibule, is less clear based on most structural studies, but this region may operate in a similar manner than that of a periplasmic constriction, regulating solute permeation in an opposite direction.

Further, it has recently been proposed that a specific pattern of residues forming ar/R/LE1-LE2 constriction regions and a precise spacing between NPA motifs control solute-conducting selectivity in plant aquaporins. A bioinformatics analysis of more than 30 aquaporins and experimental measurements of transport rates in *X.*

laevis oocytes (Deshmukh et al. 2015) revealed that permeation of silicic acid was confined to aquaporins with the Gly-Ser-Gly-Arg selectivity filter constriction signature and a precise spacing of 108 residues between NPA motifs. Notably, this Gly-Ser-Gly-Arg signature carried a low CvV value (317 $Å^3$).

To determine if an observation that a barley NIP-type aquaporin HvNIP2;1 exerts a wide solute selectivity (Schnurbusch et al. 2010) can be linked to its specific sequence and structural features, we conducted the bioinformatics analyses of 75 mono- and dicotyledonous representative sequences of NIP aquaporins (Fig. 2a). These entries (Table 1) formed three independent clades NIP-I, NIP-II and NIP-III

Table 1 The names and GenBank/NCBI accession numbers of 75 nodulin 26-like intrinsic proteins (NIPs) from listed plant species that were used in phylogeny reconstruction (cf. Fig. 2)

Name in the tree	Accession number	Species
AtNIP1-1	CAA16760.2	*Arabidopsis thaliana*
AtNIP1-2	NP_193626.1	*Arabidopsis thaliana*
AtNIP2-1	NP_180986.1	*Arabidopsis thaliana*
AtNIP3-1	NP_174472.2	*Arabidopsis thaliana*
AtNIP4-1	NP_198597.1	*Arabidopsis thaliana*
AtNIP4-2	NP_198598.1	*Arabidopsis thaliana*
AtNIP5-1	NP_192776.1	*Arabidopsis thaliana*
AtNIP6-1	NP_178191.1	*Arabidopsis thaliana*
AtNIP7-1	NP_566271.1	*Arabidopsis thaliana*
BdNIP1-1	XP_003571857.1	*Brachypodium distachyon*
BdNIP2-1	XP_003570658.1	*Brachypodium distachyon*
BdNIP2-2	XP_003564051.1	*Brachypodium distachyon*
BdNIP3-3	XP_003574178.1	*Brachypodium distachyon*
BrNIP4-3	XP_009140163.1	*Brassica rapa*
BrNIP5-1	XP_009134192.1	*Brassica rapa*
CclNIP1-1	XP_006430637.1	*Citrus clementine*
CclNIP2-1	ESR44391.1	*Citrus clementine*
CclNIP3-2	XP_006434369.1	*Citrus clementine*
CsNIP1-4	KDO63097.1	*Citrus sinensis*
CsNIP2-1	XP_006482598.1	*Citrus sinensis*
CsNIP3-2	XP_006472916.1	*Citrus sinensis*
EgNIP1-2	XP_010915460.1	*Elaeis guineensis*
EgNIP3-4	XP_010933763.1	*Elaeis guineensis*
FvNIP1-1	XP_004309621.1	*Fragaria vesca*
FvNIP2-1	XP_004304304.1	*Fragaria vesca*
FvNIP3-3	XP_004309493.1	*Fragaria vesca*
GmNIP1-2	XP_003518381.1	*Glycine max*
GmNIP2-1	XP_003534451.1	*Glycine max*
GmNIP3-1	XP_003547292.1	*Glycine max*
HvNIP2-1	BAH24163	*Hordeum vulgare*
MaNIP1-1	XP_009404528.1	*Musa acuminate*
MaNIP2-1	XP_009381416.1	*Musa acuminate*

(continued)

Table 1 (continued)

Name in the tree	Accession number	Species
MaNIP2-2	XP_009401397.1	*Musa acuminate*
MaNIP2-3	XP_009419139.1	*Musa acuminate*
MaNIP2-4	XP_009403165.1	*Musa acuminate*
MaNIP3-2	XP_009388143.1	*Musa acuminate*
OsNIP1-1	NP_001046375.1	*Oryza sativa*
OsNIP2-1	NP_001048108.1	*Oryza sativa*
OsNIP2-2	BAF19121.1	*Oryza sativa*
OsNIP3-1	Q0IWF3.2	*Oryza sativa*
PpNIP5-1a	XP_001754375.1	*Physcomitrella patens*
PpeNIP1-3	XP_007216120.1	*Prunus persica*
PpeNIP2-1	XP_007216227.1	*Prunus persica*
PpeNIP3-2	XP_007209472.1	*Prunus persica*
PtNIP1-4	XP_006372594.1	*Populus trichocarpa*
PtNIP2-1	XP_002324057.1	*Populus trichocarpa*
PtNIP3-3	XP_002298990.1	*Populus trichocarpa*
PtNIP3-4	XP_002317642.1	*Populus trichocarpa*
RcNIP1-4	XP_002532963.1	*Ricinus communis*
RcNIP2-1	XP_002534417.1	*Ricinus communis*
RcNIP3-1	XP_002518973.1	*Ricinus communis*
SbNIP1-1	XP_002453573.1	*Sorghum bicolor*
SbNIP2-1	XP_002454286	*Sorghum bicolor*
SbNIP2-2	XP_002438105.1	*Sorghum bicolor*
SbNIP3-4	XP_002464380.1	*Sorghum bicolor*
SiNIP2-1	KQL31494.1	*Setaria italic*
SiNIP2-2	KQL10018.1	*Setaria italic*
SiNIP3-1	XP_004982621.1	*Setaria italic*
SlNIP1-4	BAO18645.1	*Solanum lycopersicum*
SlNIP2-1	NP_001274283.1	*Solanum lycopersicum*
SlNIP3-2	NP_001274288.1	*Solanum lycopersicum*
SmNIP3-1	XP_002976312.1	*Selaginella moellendorffii*
SmNIP5-1	XP_002962550.1	*Selaginella moellendorffii*
StNIP1-4	XP_006344325.1	*Solanum tuberosum*
StNIP3-2	NP_001274996.1	*Solanum tuberosum*
TaNIP2-1	ADM47602	*Triticum aestivum*
VvNIP1-4	CBI33542.3	*Vitis vinifera*
VvNIP2-1	XP_002278054.2	*Vitis vinifera*
VvNIP3-2	XP_002276319.1	*Vitis vinifera*
ZmNIP1-1	AFW77428.1	*Zea mays*
ZmNIP2-1	ACF79677.1	*Zea mays*
ZmNIP2-2	ABF67956.1	*Zea mays*
ZmNIP2-3	ACG28405.1	*Zea mays*
ZmNIP2-4	AAK26849.1	*Zea mays*
ZmNIP3-3	NP_001105021.1	*Zea mays*

with different selectivity filter signatures (Mitani et al. 2008; Ma and Yamaji 2015). Members of the NIP-I clade contain Trp-Val-Ala-Arg (WVAR) and Trp-Ile-Ala-Arg (WIAR) motifs, and the NIP-II members have Ala-Ile-Ala-Arg (AIAR), Ala-Ile-Gly-Arg (AIGR) and Ala-Val-Gly-Arg (AVGR) signatures. All NIP-III members, to which the barley NIP-type aquaporin HvNIP2;1 belongs, carry an absolutely conserved Gly-Ser-Gly-Arg (GSGR) signature in their selectivity filters (Fig. 2a in green). In this analysis, we further divided members of NIP-III into two sub-clades, α-sub-clade 1 and α-sub-clade 2 (highlighted in two lighter shades of grey) containing monocotyledonous members, and β-sub-clade (highlighted in darker grey) with dicotyledonous sequences. This suggested that the monocot α-sub-clade has diversified during evolution from the dicot β-sub-clade (Fig. 2a). However, it remains to be established if this clear diversification of selectivity filter motifs can be correlated with a solute permeation specificity of individual aquaporins, classified in specific clades or sub-clades.

4.5 Chemical Filtering of Solutes, Barriers for Ion or Proton Conductance Through the Pores of Monomers and Significance of NPA Signatures

It has been suggested, based on crystallographic analyses (Murata et al. 2000; Lee et al. 2005; Ho et al. 2009; Savage et al. 2010) and corroborated by molecular dynamics simulations (Tajkhorshid et al. 2002), that two NPA motifs provide a blocking mechanism against the passage of H^+ and other ions. This mechanism is based on a unique role of Asn residues in the pore, whereby each Asn operates as a hydrogen bond donor that has the ability to polarise the orientation of central water molecules (Savage et al. 2010). In other words, NPA motifs with the macro-dipoles of neighbouring re-entrant α-helices have the ability to flip the dipole moments of water molecules at the centre of conducting pores and to disrupt a single-file chain of water molecules, thus preventing proton conductance through the Grotthuss mechanism (Agmon 1995). Dipole moments and electrostatic potentials of charged ions or protons also ensure that these would experience repulsive forces from many more accessible carbonyl oxygen atoms lining the inner regions of vestibules, selectivity filters and pore regions.

To assure that chemical filtering of solutes is in place, and barriers against ion or proton conductance through monomer pores are operating, a series of hydrogen bond donor carbonyls and other groups pre-align or preselect solute molecules in vestibules that may later be caught in the aquaporin pores. It is assumed that these solutes have already shed their water molecules (Harries et al. 2004; Sui et al. 2001; Ho et al. 2009). A relatively stronger hydrophobicity of vestibules in non-water-conducting aquaporins should improve transport rates of solutes that contain hydrophobic components, and correspondingly the more hydrophilic vestibules of canonical aquaporins would favour the preselection of water molecules (Sui et al. 2001; Savage et al. 2003;

Ho et al. 2009). It has further been proposed that these vestibules are sites for the energetically unfavourable shedding of hydration shells of water molecules from certain solutes during de-solvation, as well as for the increase of effective solute concentrations near the entry into the pore regions (Harries et al. 2004). However, the structural analyses of aquaporin vestibules revealed that central pores operate with a different molecular mechanism. The average distance between water molecules is minimal in the pore (forming a single-file water structure) because of a very high hydrophobicity, while the opposite was found to be true for the vestibule regions of aquaporins, where water adopts a bulk-like state (Han et al. 2015). Based on this premise, it was suggested that the vestibule regions could be effective drug design targets, as these regions are the sites for initial recruitment of solutes and may control their concentrations (Ho et al. 2009; Han et al. 2015). This approach could be tested using aquaporin homology models, based on structural data for closely related experimental structures, to solve the mechanistic problems of aquaporin solute selectivity and for in silico drug design.

4.6 Ion Conductance Through a Central Pore of Tetramers

While conductance of water or other neutral solutes through the central tetrameric pore has been excluded, due to its hydrophobic nature (Fu et al. 2000; Murata et al. 2000), a controversy prevails as to whether a central tetrameric pore conducts ionic species. The reason for this is that the central pore in some aquaporins may be up to 10 Å wide, considerably larger than, for example, the pore in the tetrameric KcsA potassium ion channel (Anderson et al. 1992). It was suggested that a central pore may serve as a potential path for ion permeation (Yool et al. 1996; Fu et al. 2000). To this end, the ion conductivity for a central pore in a human aquaporin has been proposed (especially after cGMP activation), and a proof-of-concept for this hypothesis was supported by molecular dynamics simulations and ion transport measurements in *X. laevis* oocytes (Yu et al. 2006). Notably, through molecular dynamics simulations, cGMP was found to interact with Arg-rich cytoplasmic loop D facilitating its outward movement, which was hypothesised to open a cytoplasmic gate and mediate ion conductance. Further, a homo-tetrameric plasma and inner chloroplast membrane PIP2;1 aquaporin from *Nicotiana tabacum* facilitated CO_2 but did not permeate water (Uehlein et al. 2008). These authors hypothesised that CO_2 could permeate through a central (so-called fifth) pore (Otto et al. 2010). The previous findings were confirmed by Wang et al. (2016), who showed that *Arabidopsis* PIP2;1 permeated CO_2, and served as a key interactor of the carbonic anhydrase βCA4. Importantly, these authors established that extracellular CO_2 signalling was linked to a SLAC1 ion channel regulation upon co-expression of PIP2;1, βCA4, SLAC1 and protein kinases. No molecular dynamics simulation studies have yet been performed on CO_2 transport. In summary, the question of whether the central tetrameric pore conducts ionic species or CO_2 is still highly contentious. This pathway must be more thoroughly investigated for its ion-conducting activity, at least in aquaporins in which the properties of the central pore are predicted to be conducive for this function.

4.7 Mutational Studies to Alter Transport Selectivity and Rates

One rapid way to investigate solute selectivity, modify transport rates, is to introduce variations in sequences (Jung et al. 1994; Jahn et al. 2004; Bienert et al. 2013; Hayes et al. 2013; Kirscht et al. 2016) and integrate both transport functional and structural observations. For over more than 20 years of this research, significant information has been gained based on the studies of wild-type and variant plant of aquaporins.

Several point mutations (His180Ala/Arg196Ala and Phe56Ala/His180Ala) in the ar/R/LE1-LE2 selectivity filter of a human water-specific aquaporin 1 allowed conversion of this orthodox water-permeable aquaporin into a more multifunctional aquaporin, permeating other solutes such as urea, glycerol and ammonia. These variations increased the maximal diameter of the constriction of the ar/R/LE1-LE2 selectivity filter by threefold (Beitz et al. 2006). However, surprisingly the Arg196Val substitution (removal of a positive charge from Arg196) allowed proton passage in both directions. Further, Beitz and co-authors (2006) established that protons did not permeate according to the Grotthuss mechanism and concluded in accordance with Zeuthen et al. (2013) that the electrostatic proton barrier in aquaporins depended on both NPA and ar/R/LE1-LE2 constrictions. These findings and those of Hub and de Groot (2008) based on molecular dynamics simulations imply that the ar/R region does not preclude water conductance but affects uncharged solutes conductance, emphasising the importance of the ar/R/LE1-LE2 residues for channel selectivity.

On the other hand, when three selectivity filter signature residues (Phe43Trp/His174Gly/Thr183Phe) of the glycerol-permeating *E. coli* aquaporin (AqpF) were introduced into its water-conducting counterpart (AqpZ), there was no increase in glycerol conductance, although a decrease of water permeability was recorded in both reciprocally mutated aquaporins (Savage et al. 2010). Notable observations were reported by Liu et al. (2005), who in a rat anion-selective aquaporin 6 substituted Asn for Gly in α-helix 2. This mutation resulted in the elimination of anion permeability but also led to elevated water transport when variant proteins were expressed in *X. laevis* oocytes. These observations indicated that each aquaporin is structurally unique and that simple variations of selectivity filter residues may not result in an altered solute selectivity. To proceed forward with designing a desired solute selectivity of aquaporins, one needs to integrate multifaceted knowledge of bioinformatics, molecular modelling and classical molecular dynamics.

Ma and co-workers (2008) investigated the substrate specificity of a rice aquaporin NIP2;1 using *X. laevis* and *Saccharomyces cerevisiae* cells. They isolated two alleles, whereby the allele lsi2-1 had lower accumulation of toxic arsenious acid than the allele lsi2-2 but a higher silicic acid uptake (see also chapter "Plant Aquaporins and Metalloids"). These metalloids differ by 0.62 Å in their atomic radii (Fig. 3), and thus it is conceivable to think that protein variants with different transport rates of essential (silicic acid) and toxic (arsenious acid) metalloids could in principle be engineered. Comparison of sequences indicated that Thr342 could be

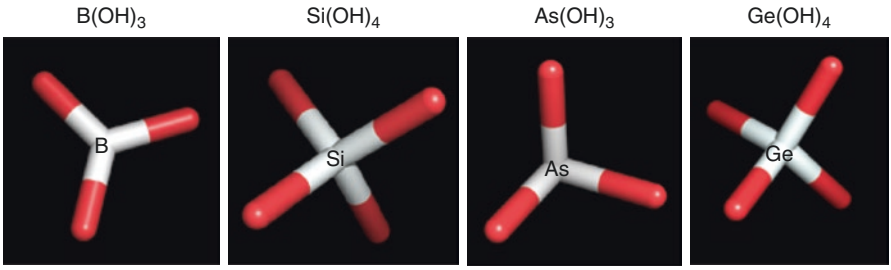

Molecular sizes of metalloids:	
B (OH)$_3$	3.43 Å
As(OH)$_3$	3.57 Å
Si (OH)$_4$	4.19 Å
Ge(OH)$_4$	4.48 Å

Fig. 3 Structures and atomic radii of metalloid molecules of boric acid [B(OH)$_3$], silicic acid [Si(OH)$_4$], arsenious acid [As(OH)$_3$] and germanic acids [Ge(OH)$_4$] that are known to be transported by the members of an α-sub-clade of NIP-III aquaporins from monocotyledonous plants. Structures are shown in stick representations. The dimensions of atomic radii are given in Å

mutated to Arg in lsi2-2 that was positioned in the membrane H6 (topology explained in Fig. 1) and not in the pore region of the lsi2-2 protein. This study was extended by Mitani-Ueno et al. (2011), who investigated whether ar/R/LE1-LE2 filter and NPA motifs could be altered to influence the solute transport selectivity of rice NIP2;1 preferring silicic over boric acid, and conversely that of Arabidopsis NIP5;1 with a reversed substrate selectivity. Both proteins also permeate arsenious acid and thus this study also carries biotechnological significance. The individual changes in rice NIP2;1 at the ar/R/LE1 positions did not alter transport of metalloids; however, the H5 mutation led to a loss of transport activity of both metalloids. Conversely, mutations in *Arabidopsis* NIP5;1 did not restore transport of silicic acid, and double mutations in H2 and H5 did not affect transport of arsenious acid. Further, Hayes et al. (2013) performed targeted mutagenesis of the specific residues within the ar/R/LE1-LE2 selectivity filter in barley NIP2;1 to alter its metalloid solute selectivity. Two of the mutations in the H2 position Gly88Ala and Gly88Cys showed a growth restoration in the presence of boric (smallest atomic radius, Fig. 3) and germanic (largest atomic radius) acids; nevertheless, the growth inhibition on arsenious acid (the second smallest atomic radius from the four metalloids) was preserved. These observations suggested that although mutations altered the substrate specificity of barley NIP2;1, metalloid permeation seemed to be controlled by other factors than simply by atomic radii of solutes. Potential controlling factors may entail differences in de-solvation rates within the vestibule regions of aquaporins *prior* to interactions with ar/R/LE1-LE2 selectivity filter residues or differences in overall interaction modes of metalloids with aquaporin molecules. These hypotheses can be tested using molecular dynamics simulation experiments.

The observations outlined above further extend a suggestion that ar/R/LE1-LE2 selectivity filter properties alone do not control solute selectivity of aquaporins and that other structural elements that do not directly interact with solutes may play essential roles in solute permeation specificity (Savage et al. 2010).

Another alternative to identify variations in protein sequences of aquaporins is to search for natural variation in cultivars that have precisely adapted to specific or stress-affected environments. These types of studies are just beginning to appear with aquaporins and other transport systems (e.g. Pallotta et al. 2014). The question then arises as to whether the responses of natural variants for specific stresses, such as drought or mineral toxicity, have already been optimised in crop and other plants through a long history of selection of native variants or are there still opportunities for a significant gain through allelic mining (Langridge et al. 2006). Although the information on natural variation of aquaporins and other transport systems involved in drought or other biotic and abiotic stresses is scarse, a few landmark studies have appeared (Pallotta et al. 2014; Hayes et al. 2015; Nagarajan et al. 2016).

5 Gating Mechanisms of Aquaporins Induced by pH, Cation Binding and Phosphorylation or Lengths of Loops and Mutational Studies

The concept of gating in plant aquaporins was proposed long before (Tyerman et al. 1989; Azaizeh et al. 1992; Tyerman et al. 1999; Yool and Weinstein 2002) both states, i.e. open and closed, of any aquaporin were elucidated at the atomic levels. Later both states of the spinach aquaporin (Fig. 1c) were defined at atomic levels in: (i) closed states at pH 8.0 (PDB ID: 1Z98; Tornroth-Horsefield et al. 2006) and pH 6.0 (PDB ID: 4IA4; Frick et al. 2013a, b) and (ii) an open state (PDB ID: 2B5F; Törnroth-Horsefield et al. 2006). Further, a so-called stochastic model of osmotic water transport was suggested, based on testing of a range of channel sizes and geometries of human aquaporins and their mutants (Zeuthen et al. 2013); this knowledge can directly be linked to the concept of gating.

Two groups of mechanisms that appear to be conserved in plant aquaporins are known to facilitate gating, i.e. the transitions between open and closed states. More precisely, the term gating refers to the opened (activated or conductive) and closed (deactivated or non-conductive) states, whereby these states represent distinct spatial conformations of the same channel. Here, that conformation interchange results in increasing the limiting size of the pore to accommodate solutes. The first group of mechanisms of gating includes pH changes, cation binding and post-translational phosphorylation (Törnroth-Horsefield et al. 2006; Frick et al. 2013a, b). The second group of gating mechanisms is based on loop lengths and their movements (Fischer et al. 2009).

The origin of gating was explored in a spinach aquaporin, for which the atomic structures of both states are available, using single and double Ser115Glu and Ser274Glu phosphorylation mimic variants (Nyblom et al. 2009). Although all

mutants crystallised in a closed conformation, the analysis revealed that neither variation mimicked the naturally occurring phosphorylated state of the protein. However, combined functional and structural analyses revealed that in the Ser115Glu variant, the neighbouring Glu31 significantly moved away from its wild-type position, leading to a disruption of the divalent cation (presumed to be Ca^{2+})-binding site that stabilises loop D. These observations highlight the fact that phosphorylation of Ser115 could induce structural rearrangements and thus control opening and closing states of the pore.

The crystal structures of a spinach aquaporin, which have been obtained in several conformational states (a water-closed state at pH 8.0 (Törnroth-Horsefield et al. 2006) and at pH 6.0 (Frick et al. 2013a, b)), revealed a closing mechanism that in the plasma membrane results from a rapid drop of cytosolic pH due to anoxia that occurs during flooding (Tournaire-Roux et al. 2003). The closing mechanism is assumed to involve the interaction of the conserved pH-sensitive His193 residue on cytosolic loop D with the divalent cation (presumed to be Ca^{2+})-binding site. Here, in a protonated state, His adopts an alternative rotameric state and interacts with Asp28 that resides on a short N-terminal α-helix. This closing mechanism is also maintained by dephosphorylation of a closely positioned Ser115 residue on loop B (Frick et al. 2013a, b).

These observations, based on structural analyses of a wild-type and variant spinach aquaporins, indicate that gating mechanisms are linked to movements of loops B and D, post-translational phosphorylating events of Ser residues, protonation states of a His residue and the involvement of a divalent cation-binding site (Törnroth-Horsefield et al. 2006). These studies emphasise the control of gating by several concurrent events to open and close a solute-conducting pore (Nyblom et al. 2009; Frick et al. 2013a, b).

The second group of gating mechanisms is based on loop lengths and their movements alone and was revealed for the first time using the full-length and truncated forms of the yeast aquaporin Aqy1 from *Pichia pastoris*, resolved to 1.15 Å (Fischer et al. 2009). Structural data revealed that the pore of the Aqy1 aquaporin was closed by its own N-terminus. Here, Tyr31 formed a hydrogen bond to a water molecule and the backbone oxygen atoms of nearby Gly residues, located in the vicinity of the pore, consequently obstructing the cytoplasmic entrance to the pore. Additional mutational studies combined with molecular dynamics simulations suggested that water flow through the pore may be regulated by specific arrangements of post-translational regulation sites by phosphorylation and also by mechanosensitive gating. The latter gating could also be related to highly curved membrane environments, where aquaporins may reside. This was confirmed by molecular dynamics simulation, indicating that Aqy1 was regulated by both surface tension and membrane curvature. This type of gating could provide a rapid pressure regulator in response to unexpected cellular shock, aiding adaptation and microbial survival (Fischer et al. 2009), as well as to plants that employ a turgor pressure (Tyerman et al. 1989, 1999).

6 The Structural Knowledge of Aquaporins Has Strategic Significance in Agricultural Biotechnology, Nanobiotechnology and Environmental Sciences

Although transport function is central to plants, limited information is available on a structural basis of the permeation function of plant aquaporins. These investigations have so far been largely driven by genetics and physiology, but the knowledge of molecular function is required if we are to modify the properties of these transport proteins (Schroeder et al. 2013; Chaumont and Tyerman 2014; Nagarajan et al. 2016). Further, modifying the properties of aquaporins depends on a detailed mechanistic knowledge of their behaviour. Even though many aquaporins have been identified, their intrinsic hydrophobic properties made these studies difficult. As of May 2016, from 615 unique membrane proteins (http://blanco.biomol.uci.edu/mpstruc/), only five structures of plant transport proteins are known. These include two aquaporins from *S. oleracea* and *A. thaliana*, a nitrate transporter and a voltage-gated two-pore channel from *A. thaliana* and a SWEET transporter from *Oryza sativa*. Thus, two unique plant aquaporin structures are those of the water-conducting SoPIP2;1 aquaporin from *S. oleracea* (in several conformational states and variant forms) and the AtTIP2;1 aquaammoniaporin from *A. thaliana* (Kirscht et al. 2016).

Surprisingly, limited information is available on solute permeation specificity of plant aquaporins, although these data in conjunction with structural information are vital strategic tools for modifying their molecular function. We therefore need detailed structural data on all subfamilies of plant aquaporins from economically important food plants such as wheat, barley, maize and rice that conduct a variety of solutes, including those of multi-selective NIPs that have importance in food security and safety (Ma et al. 2006; Schnurbusch et al. 2010; Hayes et al. 2013). Targets for this knowledge include, for example, improving the nutritional quality and safety of plant products for humans, such as exclusion of toxic arsenic from food plants (Isayenkov and Maathuis 2008; Kamiya et al. 2009; Li et al. 2011; Hayes et al. 2013; Schnurbusch et al. 2010; Xu et al. 2015). Modifying nutrient fluxes is also important for protection of plants from excessive accumulation of metalloids such as boric acid, which become toxic at high concentrations (Hayes et al. 2015; Nagarajan et al. 2016).

Uncharged ion pairs of mercury, gold, copper and cadmium are also known to perturb plant water status (Belimov et al. 2015) and have been reported to be the potent inhibitors of aquaporins that operate through cysteine-related mechanisms (Niemietz and Tyerman 2002). Heavy metal-induced perturbations of aquaporin function at the plant level have been explained by a decrease of both root and shoot hydraulic conductance, leading to decreasing leaf water potentials and turgor, which may close stomata (Zhu et al. 2005). On the other hand, many aquaporins are mercury insensitive. Remarkably Frick et al. (2013a, b) in a spinach aquaporin observed mercury-increased water permeability, using a non-cysteine-related mechanism, whereby presumably other factors affected the aquaporin; one of them could be the properties of a lipid bilayer.

Finally, an obvious potential application of aquaporins is in nanotechnology by creating stable biomimetic membranes, such as those with embedded robust aquaporin folds that have excellent separation performance and permit rapid water diffusion. Hence, a next important application of aquaporins could be in environmental sciences, more specifically in water desalination, waste-water recovery and fertiliser and soil component retrieval. Application and profitability on an industrial scale would require stable and robust aquaporin structures with highly selective permeation functions and rapid transport rates (Wang et al. 2015).

Acknowledgements This work was supported by the grants from the Australian Research Council (LP120100201 and DP120100900 to M. H.). Jay Rongala and Dr. Julie Hayes (Australian Centre for Plant Functional Genomics, University of Adelaide) are thanked for the assistance with literature and for critically reading the manuscript, respectively. I acknowledge Professor Steve Tyerman and the past members of my laboratory for insightful discussions.

References

Abascal F, Irisarri I, Zardoya R (2014) Diversity and evolution of membrane intrinsic proteins. Biochim Biophys Acta 1840:1468–1481

Agemark M, Kowal J, Kukulski W, Nordén K, Gustavsson N, Johanson U, Engel A, Kjellbom P (2012) Reconstitution of water channel function and 2D-crystallization of human aquaporin 8. Biochim Biophys Acta 1818:839–850

Agmon N (1995) The Grotthuss mechanism. Chem Phys Lett 244:456–462

Agre P, Kozono D (2003) Aquaporin water channels: molecular mechanisms for human diseases. FEBS Lett 555:72–78

Agre P, Sasaki S, Chrispeels J (1993) Aquaporins: a family of water channel proteins. Am J Physiol Ren Physiol 265:F461

Anderson JA, Huprikar SS, Kochian LV, Lucas WJ, Gaber RF (1992) Functional expression of a probable *Arabidopsis thaliana* potassium channel in *Saccharomyces cerevisiae*. Proc Natl Acad Sci U S A 89:3736–3740

Ariani A, Gepts P (2015) Genome-wide identification and characterization of aquaporin gene family in common bean (*Phaseolus vulgaris* L.). Mol Genet 290:1771–1785

Beitz E, Wu B, Holm LM, Schultz JE, Zeuthen T (2006) Point mutations in the aromatic/arginine region in aquaporin 1 allow passage of urea, glycerol, ammonia, and protons. Proc Natl Acad Sci U S A 103:269–274

Belimov AA, Dodd IC, Safronova VI, Malkov NV, Davies WJ, Tikhonovich IA (2015) The cadmium-tolerant pea (*Pisum sativum* L.) mutant SGECdt is more sensitive to mercury: assessing plant water relations. J Exp Bot 66:2359–2369

Besse M, Knipfer T, Miller AJ, Verdeil JL, Jahn TP, Fricke W (2011) Developmental pattern of aquaporin expression in barley (*Hordeum vulgare* L.) leaves. J Exp Bot 62:4127–4142

Besserer A, Burnotte E, Bienert GP, Chevalier AS, Errachid A, Grefen C, Blatt MR, Chaumont F (2012) Selective regulation of maize plasma membrane aquaporin trafficking and activity by the SNARE SYP121. Plant Cell 24:3463–3481

Bienert GP, Bienert MD, Jahn TP, Boutry M, Chaumont F (2011) Solanaceae XIPs are plasma membrane aquaporins that facilitate the transport of many uncharged substrates. Plant J 66:306–317

Bienert GP, Desguin B, Chaumont F, Hols P (2013) Channel-mediated lactic acid transport: a novel function for aquaglyceroporins in bacteria. Biochem J 454:559–570

Borgnia M, Nielsen S, Engel A, Agre P (1999) Cellular and molecular biology of the aquaporin water channels. Annu Rev Biochem 68:425–458

Chaumont F, Tyerman SD (2014) Aquaporins: highly regulated channels controlling plant water relations. Plant Physiol 164:1600–1618
Chaumont F, Barrieu F, Wojcik E, Chrispeels MJ, Jung R (2001) Aquaporins constitute a large and highly divergent protein family in maize. Plant Physiol 125:1206–1215
Choi WG, Roberts DM (2007) *Arabidopsis* NIP2;1, a major intrinsic protein transporter of lactic acid induced by anoxic stress. J Biol Chem 282:24209–24218
Cordeiro RM (2015) Molecular dynamics simulations of the transport of reactive oxygen species by mammalian and plant aquaporins. Biochim Biophys Acta 1850:1786–1794
Deshmukh RK, Vivancos J, Ramakrishnan G, Guérin V, Carpentier G, Sonah H, Labbé C, Isenring P, Belzile FJ, Bélanger RR (2015) A precise spacing between the NPA domains of aquaporins is essential for silicon permeability in plants. Plant J 83:489–500
Diehn TA, Pommerrenig B, Bernhardt N, Hartmann A, Bienert GP (2015) Genome-wide identification of aquaporin encoding genes in *Brassica oleracea* and their phylogenetic sequence comparison to *Brassica* crops and *Arabidopsis*. Front Plant Sci 6:166. doi:10.3389/fpls.2015.00166
Dordas C, Chrispeels MJ, Brown PH (2000) Permeability and channel-mediated transport of boric acid across membrane vesicles isolated from squash roots. Plant Physiol 124:1349–1362
Dynowski M, Schaaf G, Loque D, Moran O, Ludewig U (2008) Plant plasma membrane water channels conduct the signalling molecule H_2O_2. Biochem J 414:53–61
Eriksson UK, Fischer G, Friemann R, Enkavi G, Tajkhorshid E, Neutze R (2013) Subangstrom resolution X-ray structure details aquaporin-water interactions. Science 340:1346–1349
Fang X, Yang B, Matthay MA, Verkman AS (2002) Evidence against aquaporin-1-dependent CO_2 permeability in lung and kidney. J Physiol 542:63–69
Fischer G, Kosinska-Eriksson U, Aponte-Santamaría C, Palmgren M, Geijer C, Hedfalk K, Hohmann S, de Groot BL, Neutze R, Lindkvist-Petersson K (2009) Crystal structure of a yeast aquaporin at 1.15 angstrom reveals a novel gating mechanism. PLoS Biol 7:e1000130
Fotiadis D, Hasler L, Muller DJ, Stahlberg H, Kistler J, Engel A (2000) Surface tongue-and-groove contours on lens MIP facilitate cell-to-cell adherence. J Mol Biol 300:779–789
Fotiadis D, Jenö P, Mini T, Wirtz S, Müller SA, Fraysse L, Kjellbom P, Engel A (2001) Structural characterization of two aquaporins isolated from native spinach leaf plasma membranes. J Biol Chem 276:1707–1714
Frick A, Järvå M, Ekvall M, Uzdavinys P, Nyblom M, Törnroth-Horsefield S (2013a) Mercury increases water permeability of a plant aquaporin through a non-cysteine-related mechanism. Biochem J 454:491–499
Frick A, Järvå M, Törnroth-Horsefield S (2013b) Structural basis for pH gating of plant aquaporins. FEBS Lett 587:989–993
Frick A, Eriksson UK, de Mattia F, Oberg F, Hedfalk K, Neutze R, de Grip WJ, Deen PM, Törnroth-Horsefield S (2014) X-ray structure of human aquaporin 2 and its implications for nephrogenic diabetes insipidus and trafficking. Proc Natl Acad Sci U S A 111:6305–6310
Fricke W, McDonald AJ, Mattson-Djos L (1997) Why do leaves and leaf cells of *N*-limited barley elongate at reduce rate? Planta 202:522–530
Fu D, Libson A, Miercke LJ, Weitzman C, Nollert P, Krucinski J, Stroud RM (2000) Structure of a glycerol-conducting channel and the basis for its selectivity. Science 290:481–486
Gao Z, He X, Zhao B, Zhou C, Liang Y, Ge R, Shen Y, Huang Z (2010) Overexpressing a putative aquaporin gene from wheat, *TaNIP*, enhances salt tolerance in transgenic *Arabidopsis*. Plant Cell Physiol 51:767–775
Gomes D, Agasse A, Thiébaud P, Delrot S, Gerós H, Chaumont F (2009) Aquaporins are multifunctional water and solute transporters highly divergent in living organisms. Biochim Biophys Acta 1788:1213–1228
Gonen T, Sliz P, Kistler J, Cheng Y, Walz T (2004) Aquaporin-0 membrane junctions reveal the structure of a closed water pore. Nature 429:193–197
Gonen T, Cheng Y, Sliz P, Hiroaki Y, Fujiyoshi Y, Harrison SC, Walz T (2005) Lipid-protein interactions in double-layered two-dimensional AQP0 crystals. Nature 438:633–368
Gorin MB, Yancey SB, Cline J, Revel JP, Horwitz J (1984) The major intrinsic protein (MIP) of the bovine lens fiber membrane: characterization and structure based on cDNA cloning. Cell 39:49–59

Gupta AB, Sankararamakrishnan R (2009) Genome-wide analysis of major intrinsic proteins in the tree plant *Populus trichocarpa*: characterization of XIP subfamily of aquaporins from evolutionary perspective. BMC Plant Biol 9:134. doi:10.1186/1471-2229-9-134

Gupta AB, Verma RK, Agarwal V, Vajpai M, Bansal V, Sankararamakrishnan R (2012) MIPModDB: a central resource for the superfamily of major intrinsic proteins. Nucleic Acids Res 40: D362–D369

Han C, Tang D, Kim D (2015) Molecular dynamics simulation on the effect of pore hydrophobicity on water transport through aquaporin-mimic nanopores. Colloids Surf A Physicochem Eng Asp 481:38–42

Harries WE, Akhavan D, Miercke LJ, Khademi S, Stroud RM (2004) The channel architecture of aquaporin 0 at a 2.2-Å resolution. Proc Natl Acad Sci USA 101:14045–14050

Hayes JE, Pallotta M, Baumann U, Berger B, Langridge P, Sutton T (2013) Germanium as a tool to dissect boron toxicity effects in barley and wheat. Funct Plant Biol 40:618–627

Hayes JE, Pallotta M, Garcia M, Öz MT, Rongala J, Sutton T (2015) Diversity in boron toxicity tolerance of Australian barley (*Hordeum vulgare* L.) genotypes. BMC Plant Biol 15:231–234

Ho JD, Yeh R, Sandstrom A, Chorny I, Harries WE, Robbins RA, Miercke LJ, Stroud RM (2009) Crystal structure of human aquaporin 4 at 1.8 Å and its mechanism of conductance. Proc Natl Acad Sci USA 106:7437–7442

Höfte H, Hubbard L, Reizer J, Ludevid D, Herman EM, Chrispeels MJ (1992) Vegetative and seed-specific forms of tonoplast intrinsic protein in the vacuolar membrane of *Arabidopsis thaliana*. Plant Physiol 99:561–570

Horsefield R, Nordén K, Fellert M, Backmark A, Törnroth-Horsefield S, Terwisscha van Scheltinga AC, Kvassman J, Kjellbom P, Johanson U, Neutze R (2008) High-resolution X-ray structure of human aquaporin 5. Proc Natl Acad Sci U S A 105:13327–13332

Hove RM, Ziemann M, Bhave M (2015) Identification and expression analysis of the Barley (*Hordeum vulgare* L.) Aquaporin Gene Family. PLoS ONE 10:e0128025

Hu W, Yuan Q, Wang Y, Cai R, Deng X, Wang J, Zhou S, Chen M, Chen L, Huang C, Ma Z, Yang G, He G (2012) Overexpression of a wheat aquaporin gene, TaAQP8, enhances salt stress tolerance in transgenic tobacco. Plant Cell Physiol 53:2127–2141

Hub JS, de Groot BL (2008) Mechanism of selectivity in aquaporins and aquaglyceroporins. Proc Natl Acad Sci U S A 105:1198–1203

Isayenkov SV, Maathuis FJM (2008) The *Arabidopsis thaliana* aquaglyceroporin AtNIP7;1 is a pathway for arsenite uptake. FEBS Lett 582:1625–1628

Jahn TP, Møller AL, Zeuthen T, Holm LM, Klaerke DA, Mohsin B, Kühlbrandt W, Schjoerring JK (2004) Aquaporin homologues in plants and mammals transport ammonia. FEBS Lett 574: 31–36

Johanson U, Karlsson M, Johansson I, Gustavsson S, Sjövall S, Fraysse L, Weig AR, Kjellbom P (2001) The complete set of genes encoding major intrinsic proteins in *Arabidopsis* provides a framework for a new nomenclature for major intrinsic proteins in plants. Plant Physiol 126:1358–1369

Johnson KD, Höfte H, Chrispeels MJ (1990) An intrinsic tonoplast protein of protein storage vacuoles in seeds is structurally related to a bacterial solute transporter (GIpF). Plant Cell 2:525–532

Jung JS, Preston GM, Smith BL, Guggino WB, Agre P (1994) Molecular structure of the water channel through aquaporin CHIP. The hourglass model. J Biol Chem 269:14648–14654

Kamiya T, Tanaka M, Mitani N, Ma JF, Maeshima M, Fujiwara T (2009) NIP1;1, an aquaporin homolog, determines the arsenite sensitivity of *Arabidopsis thaliana*. J Biol Chem 284:2114–2120

Kirscht A, Kaptan SS, Bienert KP, Chaumont F, Nissen P, de Groot BL, Kjellbom P, Gourdon P, Johanson U (2016) Crystal structure of an ammonia-permeable aquaporin. PLoS Biol 14:e1002411

Kitchen P, Conner AC (2015) Control of the aquaporin-4 channel water permeability by structural dynamics of Aromatic/Arginine selectivity filter residues. Biochemistry (USA) 54:6753–6755

Langridge P, Paltridge N, Fincher G (2006) Functional genomics of abiotic stress tolerance in cereals. Brief Funct Genomic Proteomic 4:343–354

Lee KJ, Kozono D, Remis J, Kitagawa Y, Agre P, Stroud RM (2005) Structural basis for conductance by the archaeal aquaporin AqpM at 1.68Å. Proc Natl Acad Sci USA 102:18932–18937

Li T, Choi WG, Wallace IS, Baudry J, Roberts DM (2011) *Arabidopsis thaliana* NIP7;1: an anther-specific boric acid transporter of the aquaporin superfamily regulated by an unusual tyrosine in helix 2 of the transport pore. Biochemistry 50:6633–6641

Li G, Santoni V, Maurel C (2014) Plant aquaporins: roles in plant physiology. Biochim Biophys Acta 1840:1574–1582

Li J, Ban L, Wen H, Wang Z, Dzyubenko N, Chapurin V, Gao H, Wang X (2015) An aquaporin protein is associated with drought stress tolerance. Biochem Biophys Res Commun 459:208–213

Liu L-H, Ludewig U, Gassert B, Frommer WB, von Wirén N (2003) Urea transport by nitrogen-regulated tonoplast intrinsic proteins in *Arabidopsis*. Plant Physiol 133:1220–1228

Liu K, Kozono D, Kato Y, Agre P, Hazama A, Yasui M (2005) Conversion of aquaporin 6 from an anion channel to a water-selective channel by a single amino acid substitution. Proc Natl Acad Sci U S A 102:2192–2197

Liu Q, Wang H, Zhang Z, Wu J, Feng Y, Zhu Z (2009) Divergence in function and expression of the NOD26-like intrinsic proteins in plants. BMC Genomics 10:313. doi:10.1186/1471-2164-10-313

Lopez D, Bronner G, Brunel N, Auguin D, Bourgerie S, Brignolas F, Carpin S, Tournaire-Roux C, Maurel C, Fumanal B, Martin F, Sakr S, Label P, Julien JL, Gousset-Dupont A, Venisse JS (2012) Insights into Populus XIP aquaporins: evolutionary expansion, protein functionality, and environmental regulation. J Exp Bot 63:2217–2230

Loqué D, Ludewig U, Yuan L, von Wirén N (2005) Tonoplast intrinsic proteins AtTIP2;1 and AtTIP2;3 facilitate NH_3 transport into the vacuole. Plant Physiol 137:671–680

Ma JF, Yamaji N (2015) A cooperative system of silicon transport in plants. Trends Plant Sci 20:435–442

Ma JF, Tamai K, Yamaji N, Mitani N, Konishi S, Katsuhara M, Ishiguro M, Murata Y, Yano M (2006) A silicon transporter in rice. Nature 440:688–691

Ma JF, Yamaji N, Mitani N, Xu XY, Su YH, McGrath SP, Zhao FJ (2008) Transporters of arsenite in rice and their role in arsenic accumulation in rice grain. Proc Natl Acad Sci U S A 105:9931–9935

Maurel C, Reizer J, Schroeder JI, Chrispeels MJ (1993) The vacuolar membrane protein gamma-TIP creates water specific channels in *Xenopus oocytes*. EMBO J 12:2241–2247

Maurel C, Verdoucq L, Luu DT, Santoni V (2008) Plant aquaporins: membrane channels with multiple integrated functions. Annu Rev Plant Biol 59:595–624

Mitani-Ueno N, Yamaji N, Zhao FJ, Ma JF (2011) The aromatic/arginine selectivity filter of NIP aquaporins plays a critical role in substrate selectivity for silicon, boron, and arsenic. J Exp Bot 62:4391–4398

Mori IC, Rhee J, Shibasaka M, Sasano S, Kaneko T, Horie T, Katsuhara M (2014) CO_2 transport by PIP2 aquaporins of barley. Plant Cell Physiol 55:251–257

Moshelion M, Moran N, Chaumont F (2004) Dynamic changes in the osmotic water permeability of protoplast plasma membrane. Plant Physiol 135:2301–2317

Mukhopadhyay R, Bhattacharjee H, Rosen BP (2014) Aquaglyceroporins: generalized metalloid channels. Biochim Biophys Acta 1840:1583–1591

Murata K, Mitsuoka K, Hirai T, Walz T, Agre P, Heymann JB, Engel A, Fujiyoshi Y (2000) Structural determinants of water permeation through aquaporin-1. Nature 407:599–605

Nagarajan Y, Rongala J, Luang S, Shadiac N, Hayes J, Sutton T, Gilliham M, Tyerman SD, McPhee G, Voelcker NH, Mertens HDT, Kirby NM, Sing A, Lee J-G, Yingling YG, Hrmova M (2016) A barley efflux transporter operates in a Na^+-dependent manner, as revealed by a multidisciplinary platform. Plant Cell 28:202–218

Newby ZE, O'Connell J 3rd, Robles-Colmenares Y, Khademi S, Miercke LJ, Stroud RM (2008) Crystal structure of the aquaglyceroporin PfAQP from the malarial parasite Plasmodium falciparum. Nat Struct Mol Biol 15:619–625

Niemietz CM, Tyerman SD (1997) Characterization of water channels in wheat root membrane vesicles. Plant Physiol 115:561–567

Niemietz CM, Tyerman SD (2002) New potent inhibitors of aquaporins: silver and gold compounds inhibit aquaporins of plant and human origin. FEBS Lett 531:443–447
Noronha H, Agasse A, Martins AP, Berny MC, Gomes D, Zarrouk O, Thiebaud P, Delrot S, Soveral G, Chaumont F, Gerós H (2014) The grape aquaporin VvSIP1 transports water across the ER membrane. J Exp Bot 65:981–993
Nyblom M, Frick A, Wang Y, Ekvall M, Hallgren K, Hedfalk K, Neutze R, Tajkhorshid E, Törnroth-Horsefield S (2009) Structural and functional analysis of SoPIP2;1 mutants adds insight into plant aquaporin gating. J Mol Biol 387:653–668
Otto B, Uehlein N, Sdorra S, Fischer M, Ayaz M, Belastegui-Macadam X, Heckwolf M, Lachnit M, Pede N, Priem N, Reinhard A, Siegfart S, Urban M, Kaldenhoff R (2010) Aquaporin tetramer composition modifies the function of tobacco aquaporins. J Biol Chem 285: 31253–31260
Pallotta M, Schnurbusch T, Hayes J, Hay A, Baumann U, Paull J, Langridge P, Sutton T (2014) Molecular basis of adaptation to high soil boron in wheat landraces and elite cultivars. Nature 514:88–91
Pandey B, Sharma P, Pandey DM, Sharma I, Chatrath R (2013) Identification of new aquaporin genes and single nucleotide polymorphism in bread wheat. Evol Bioinformatics Online 9:437–452
Park W, Scheffler BE, Bauer PJ, Campbell BT (2010) Identification of the family of aquaporin genes and their expression in upland cotton (*Gossypium hirsutum* L.). BMC Plant Biol 10:142. doi:10.1186/1471-2229-10-142
Pei J, Grishin NV (2014) PROMALS3D: multiple protein sequence alignment enhanced with evolutionary and three-dimensional structural information. Methods Mol Biol 1079:263–271
Preston GM, Carroll TP, Guggino WB, Agre P (1992) Appearance of water channels in *Xenopus oocytes* expressing red cell CHIP28 protein. Science 256:385–387
Ramahaleo T, Alexandre J, Lassalles JP (1996) Stretch activated channels in plant cells. A new model for osmoelastic coupling. Plant Physiol Biochem 34:327–334
Reddy PS, Rao TSRB, Sharma KK, Vadez V (2015) Genome-wide identification and characterization of the aquaporin gene family in *Sorghum bicolor* (L.). Plant Gene 1:18–28
Reuscher S, Akiyama M, Mori C, Aoki K, Shibata D, Shiratake K (2013) Genome-wide identification and expression analysis of aquaporins in tomato. PLoS ONE 8:e79052
Rivers RL, Dean RM, Chandy G, Hall JE, Roberts DM, Zeidel ML (1997) Functional analysis of nodulin 26, an aquaporin in soybean root nodule symbiosomes. J Biol Chem 272: 16256–16261
Saier MH, Reddy VS, Tsu BV, Ahmed MS, Li C, Moreno-Hagelsieb G (2016) The transporter classification database (TCDB). Nucleic Acids Res 44:D372–D379
Sakurai J, Ishikawa F, Yamaguchi T, Uemura M, Maeshima M (2005) Identification of 33 rice aquaporin genes and analysis of their expression and function. Plant Cell Physiol 46: 1568–1577
Sandal NN, Marcker KA (1988) Soybean nodulin 26 is homologous to the major intrinsic protein of the bovine lens fiber membrane. Nucleic Acids Res 16:9347
Savage DF, Egea PF, Robles-Colmenares Y, O'Connell JD 3rd, Stroud RM (2003) Architecture and selectivity in aquaporins: 2.5Å X-ray structure of aquaporin Z. PLoS Biol 1:E72
Savage DF, O'Connell JD 3rd, Miercke LJ, Finer-Moore J, Stroud RM (2010) Structural context shapes the aquaporin selectivity filter. Proc Natl Acad Sci U S A 107:17164–17169
Schnurbusch T, Hayes J, Hrmova M, Baumann U, Ramesh SA, Tyerman SD, Langridge P, Sutton T (2010) Boron toxicity tolerance in barley through reduced expression of the multifunctional aquaporin HvNIP2;1. Plant Physiol 153:1706–1715
Schroeder JI, Delhaize E, Frommer WB, Guerinot ML, Harrison MJ, Herrera-Estrella L, Horie T, Kochian LV, Munns R, Nishizawa NK, Tsay YF, Sanders D (2013) Using membrane transporters to improve crops for sustainable food production. Nature 497:60–66
Shelden MC, Howitt SM, Kaiser BN, Tyerman SD (2009) Identification and functional characterisation of aquaporins in the grapevine. Funct Plant Biol 36:1065–1078

Sui H, Han BG, Lee JK, Walian P, Jap BK (2001) Structural basis of water-specific transport through the AQP1 water channel. Nature 414:872–878

Tajkhorshid E, Nollert P, Jensen MO, Miercke LJ, O'Connell J, Stroud RM, Schulten K (2002) Control of the selectivity of the aquaporin water channel family by global orientational tuning. Science 296:525–530

Takano J, Wada M, Ludewig U, Schaaf G, von Wirén N, Fujiwara T (2006) The *Arabidopsis* major intrinsic protein NIP5;1 is essential for efficient boron uptake and plant development under boron limitation. Plant Cell 18:1498–1509

Tombuloglu H, Ozean I, Tombuloglu G, Sakcali S, Unver T (2015) Aquaporins in boron-tolerant barley: identification, characterization, and expression analysis. Plant Mol Biol Report. doi:10.1007/s11105-015-0930-6

Törnroth-Horsefield S, Wang Y, Hedfalk K, Johanson U, Karlsson M, Tajkhorshid E, Neutze R, Kjellbom P (2006) Structural mechanism of plant aquaporin gating. Nature 439:688–694

Tournaire-Roux C, Sutka M, Javot H, Gout E, Gerbeau P, Luu DT, Bligny R, Maurel C (2003) Cytosolic pH regulates root water transport during anoxic stress through gating of aquaporins. Nature 425:393–397

Tsukaguchi H, Shayakul C, Berger UV, Mackenzie B, Devidas S, Guggino WB, van Hoek AN, Hediger MA (1998) Molecular characterization of a broad selectivity neutral solute channel. J Biol Chem 273:24737–24743

Tsukaguchi H, Weremowicz S, Morton CC, Hediger MA (1999) Functional and molecular characterization of the human neutral solute channel aquaporin-9. Am J Phys 277:F685–F696

Tyerman SD, Oats P, Gibbs J, Dracup M, Greenway H (1989) Turgor-volume regulation and cellular water relations of *Nicotiana tabacum* roots grown in high salinities. Aust J Plant Physiol 16:517–531

Tyerman SD, Bohnert HJ, Maurel C, Steudle E, Smith JA (1999) Plant aquaporins: their molecular biology, biophysics and significance for plant water relations. J Exp Bot 50:1055–1071

Uehlein N, Lovisolo C, Siefritz F, Kaldenhoff R (2003) The tobacco aquaporin NtAQP1 is a membrane CO_2 pore with physiological functions. Nature 425:734–737

Uehlein N, Otto B, Hanson DT, Fischer M, McDowell N, Kaldenhoff R (2008) Function of *Nicotiana tabacum* aquaporins as chloroplast gas pores challenges the concept of membrane CO2 permeability. Plant Cell 20:648–657

Venkatesh J, Yu JW, Gaston D, Park SW (2015) Molecular evolution and functional divergence of X-intrinsic protein genes in plants. Mol Gen Genomics 290:443–460

Verdoucq L, Grondin A, Maurel C (2008) Structure-function analysis of plant aquaporin AtPIP2;1 gating by divalent cations and protons. Biochem J 415:409–416

Verkman AS, Mitra AK (2000) Structure and function of aquaporin water channels. Am J Physiol Ren Physiol 278:F13–F28

Verma RK, Prabh ND, Sankararamakrishnan R (2015) Intra-helical salt-bridge and helix destabilizing residues within the same helical turn: Role of functionally important loop E half-helix in channel regulation of major intrinsic proteins. Biochim Biophys Acta 1848:1436–1449

Viadiu H, Gonen T, Walz T (2007) Projection map of aquaporin-9 at 7 Å resolution. J Mol Biol 367:80–88

Wallace IS, Roberts DM (2004) Homology modeling of representative subfamilies of Arabidopsis major intrinsic proteins. Classification based on the aromatic/arginine selectivity filter. Plant Physiol 135:1059–1068

Wang Y, Schulten K, Tajkhorshid E (2005) What makes an aquaporin a glycerol channel? A comparative study of AqpZ and GlpF. Structure 13:1107–1118

Wang M, Wang Z, Wang X, Wang S, Ding W, Gao C (2015) Layer-by-layer assembly of aquaporin Z-incorporated biomimetic membranes for water purification. Environ Sci Technol 49:3761–3768

Wang C, Hu H, Qin X, Zeise B, Xu D, Rappel WJ, Boron WF, Schroeder JI (2016) Reconstitution of CO_2 regulation of SLAC1 anion channel and function of CO_2-permeable PIP2;1 aquaporin as CARBONIC ANHYDRASE4 interactor. Plant Cell 28:568–582

Weaver DC, Shomer NH, Louis CF, Roberts DM (1994) Nodulin 26, a nodule-specific symbiosome membrane protein from soybean, is an ion channel. J Biol Chem 269:17858–17862

Wudick MM, Li X, Valentini V, Geldner N, Chory J, Lin J, Maurel C, Luu DT (2015) Subcellular redistribution of root aquaporins induced by hydrogen peroxide. Mol Plant 8:1103–1114

Xu C, Wang M, Zhou L, Quan T, Xia G (2013) Heterologous expression of the wheat aquaporin gene *TaTIP2;2* compromises the abiotic stress tolerance of *Arabidopsis thaliana*. PLoS ONE 8:e79618

Xu Y, Hu W, Liu J, Zhang J, Jia C, Miao H, Xu B, Jin Z (2014) A banana aquaporin gene, *MaPIP1;1*, is involved in tolerance to drought and salt stresses. BMC Plant Biol 14:59

Xu W, Dai W, Yan H, Li S, Shen H, Chen Y, Xu H, Sun Y, He Z, Ma M (2015) *Arabidopsis* NIP3;1 plays an important role in arsenic uptake and root-to-shoot translocation under arsenite stress conditions. Mol Plant 8:722–733

Ye RG, Verkman AS (1989) Simultaneous optical measurement of osmotic and diffusional water permeability in cells and liposomes. Biochemistry 28:824–829

Yool AJ, Weinstein AM (2002) New roles for old holes: ion channel function in aquaporin-1. News Physiol Sci 17:68–72

Yool AJ, Stamer WD, Regan JW (1996) Forskolin stimulation of water and cation permeability in aquaporin 1 water channels. Science 273:1216–1218

Yu J, Yool AJ, Schulten K, Tajkhorshid E (2006) Mechanism of gating and ion conductivity of a possible tetrameric pore in aquaporin-1. Structure 14:1411–1423

Zardoya R, Ding X, Kitagawa Y, Chrispeels MJ (2002) Origin of plant glycerol transporters by horizontal gene transfer and functional recruitment. Proc Natl Acad Sci U S A 99: 14893–14896

Zeidel ML, Ambudkar SV, Smith BL, Agre P (1992) Reconstitution of functional water channels in liposomes containing purified red cell CHIP28 protein. Biochemistry 31:7436–7440

Zeuthen T, Alsterfjord M, Beitz E, MacAulay N (2013) Osmotic water transport in aquaporins: evidence for a stochastic mechanism. J Physiol 591:5017–5029

Zhang da Y, Ali Z, Wang CB, Xu L, Yi JX, Xu ZL, Liu XQ, He XL, Huang YH, Khan IA, Trethowan RM, Ma HX (2013) Genome-wide sequence characterization and expression analysis of major intrinsic proteins in soybean (*Glycine max* L.). PLoS ONE 8:e56312

Zhang J, Deng Z, Cao S, Wang X, Zhang A, Zhang X (2008) Isolation of six novel aquaporin genes from *Triticum aestivum* L. and functional analysis of *TaAQP6* in water redistribution. Plant Mol. Biol Reprod 26:32–45

Zhao XQ, Mitani N, Yamaji N, Shen RF, Ma JF (2010) Involvement of silicon influx transporter OsNIP2;1 in selenite uptake in rice. Plant Physiol 153:1871–1877

Zhu R, Macfie SM, Ding Z (2005) Cadmium-induced plant stress investigated by scanning electrochemical microscopy. J Exp Bot 56:2831–2838